PROCEEDINGS OF SCIENCE

Cosmic ray proton energy spectrum below the Knee observed by the GRAPES-3 experiment

F. Varsi,[a,*] S. Ahmad,[b] M. Chakraborty,[c] A. Chandra,[b] S. R. Dugad,[c] U. D. Goswami,[d] S. K. Gupta,[c] B. Hariharan,[c] Y. Hayashi,[e] P. Jagadeesan,[c] A. Jain,[c] P. Jain,[a] S. Kawakami,[e] H. Kojima,[f] S. Mahapatra,[g] P. K. Mohanty,[c] R. Moharana,[h] Y. Muraki,[i] P. K. Nayak,[c] T. Nonaka,[j] A. Oshima,[f] B. P. Pant,[h] D. Pattanaik,[c,g] G. S. Pradhan,[k] M. Rameez,[c] K. Ramesh,[c] L. V. Reddy,[c] S. Saha,[a] R. Sahoo,[k] R. Scaria,[k] S. Shibata[f] and M. Zuberi[c] for the GARPES-3 collaboration

[a] *Indian Institute of Technology Kanpur, Kanpur 208016, India*
[b] *Aligarh Muslim University, Aligarh 202002, India*
[c] *Tata Institute of Fundamental Research, Homi Bhabha Road, Mumbai 400005, India*
[d] *Dibrugarh University, Dibrugarh 786004, India*
[e] *Graduate School of Science, Osaka City University, Sugimoto, Sumiyoshi, Osaka 558-8585, Japan*
[f] *College of Engineering, Chubu University, Kasugai, Aichi 487-8501, Japan*
[g] *Utkal University, Bhubaneshwar 751004, India*
[h] *Indian Institute of Technology Jodhpur, Jodhpur 342037, India*
[i] *Institute for Space-Earth Environmental Research, Nagoya University, Nagoya 464-8601, Japan*
[j] *Institute for Cosmic Ray Research, Tokyo University, Kashiwa, Chiba 277-8582, Japan*
[k] *Indian Institute of Technology Indore, Indore 453552, India*

E-mail: fahim@iitk.ac.in

The GRAPES-3 experiment consists of a densely packed array of 400 plastic scintillator detectors and a large area (560 m^2) muon telescope. It measures cosmic rays in an energy range of several TeV to over 10 PeV with a trigger efficiency of more than 90% for proton primaries above 40 TeV, providing a substantial overlap with space based direct experiments. The scintillator array records the particle density and arrival time of the shower secondaries, which were used to estimate the shower parameters. The muon telescope is dedicated to recording the muon component in the shower. The observed muon multiplicity distributions (MMDs) were used for precise measurements of the average nuclear composition for proton, helium, nitrogen, aluminium, and iron primaries, independent of making assumptions about the primary composition. In the present work, Gold's unfolding algorithm was used to extract the nuclear composition and obtain the proton energy spectrum with the help of simulation based on QGSJET-II-04/FLUKA hadronic interaction models. Details of the analysis and results for the extracted composition and proton energy spectrum below the Knee will be presented.

38th International Cosmic Ray Conference (ICRC2023)
26 July - 3 August, 2023
Nagoya, Japan

*Speaker

PoS(ICRC2023)520

1. The GRAPES-3 experiment

The GRAPES-3 experiment is situated in Ooty, India, at coordinates 11.4° N, 76.7° E and an altitude of 2200 m a.s.l. It is designed to study the Primary Cosmic Rays (PRCs) from several TeV to over 10 PeV, providing a substantial overlap with direct experiments, and precisely measure their mass composition and energy spectrum. It records approximately 3×10^6 Extensive Air Showers (EASs) per day. The GRAPES-3 experiment consists of two distinct detector systems. The first detector system is comprised of a densely packed array of 400 plastic scintillator detectors [1, 2], each with an area of 1 m^2, with an inter-detector separation of 8 m. The scintillator detectors cover an area of 25000 m^2 and are organized in a hexagonal configuration to ensure the uniform detection of the EAS secondary particles across the entire array. Figure 1 displays a schematic of the GRAPES-3 EAS array, with each solid blue triangle representing the scintillator detector. It samples the charge component of the EAS and records the particle densities and arrival time of EAS secondary particles.

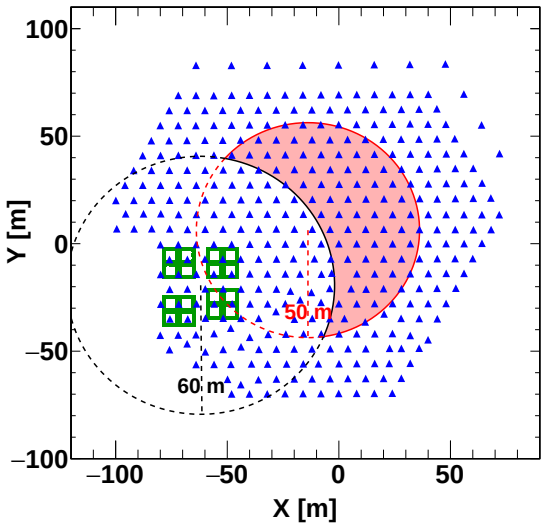

Figure 1: Schematic of GRAPES-3 EAS array. Plastic scintillator detectors (▲), tracking muon telescope modules (□) and fiducial area (- - -) are shown.

The second detector system is a large area (560 m^2) muon telescope [3] that consists of sixteen similar independent muon modules, represented by open green squares in Figure 1. The muon telescope consists of a total of 3712 proportional counters (PRCs), each of length 600 cm and cross-section area of 10 cm × 10 cm. Each muon module is composed of four layers of PRCs that are arranged in an orthogonal configuration to each other. The top absorber shields the electromagnetic and hadronic component of the EAS and offers an energy threshold of 1 GeV sec(θ) to muons that incident at a zenith angle θ. The GRAPES-3 muon telescope is sensitive to the mass composition of PCRs through muon multiplicity distribution (MMD). In Figure 1, the red-filled region depicts the fiducial area used for this analysis.

2. Reconstruction of EAS parameters and muon tracks

For each triggered EAS, the parameters such as core location (X_c, Y_c), size (N_e), and age (s) are obtained by minimizing the observed lateral distribution of particles densities in different scintillator detectors with the Nishimura-Kamata-Greisen (NKG) function. The initial estimate of arrival direction (θ, ϕ) is measured by fitting the relative arrival time of secondary particles recorded by different scintillator detectors with a plane front, followed by correction for the shower front curvature based on shower size and age to obtain a more accurate EAS direction [4]. The muon tracks, which is a statistical measure of the number of detected muons, are reconstructed by utilizing

the PRCs hit information associated with an EAS. The procedure of muon track reconstruction is explained elsewhere [5].

3. Selection quality cuts and experimental data summary

The following selection cuts are used to ensure good quality of data used in this analysis and minimize systematic uncertainties. (1)The EASs with successful parameters, arrival direction, and muon tracks are used. (2) The shower cores are restricted to a circular area of radius 50 m from the center of the array to downsize the contribution of the EAS, with improperly reconstructed shower cores, due to the core landing near the edge or outside the array. (3) Subsequently, the shower cores landing beyond a distance of 60 m from the center of the array are selected to reduce the effect of the hadron punch-through to less than 2% [5]. (4) The shower age parameter is restricted between 0.02 and 1.98 to avoid improper reconstruction due to the shower age parameter converging to its limits. (5) The zenith angle is confined to 18° to minimize the systematic uncertainty due to inclined EASs. (6) To ensure more than 90% trigger efficiency, the EASs having shower size $\geq 10^4$ are used. Data collected by the GRAPES-3 experiment in duration from 1 January 2014 to 26 October 2015 (nearly 22 months) is used for this analysis, with a total set of 1.75×10^9 EASs. The total live time of data collection is approximately 460 days. The number of EASs remaining after applying all the quality cuts is 7.81×10^7.

4. MC simulations

EAS data for five primary groups, namely proton (H), helium (He), nitrogen (N), aluminium (Al), and iron (Fe), is simlated by using CORSIKA (version 7.6900) package. The N, Al, and Fe are used to represent light (C, N, O), medium (Mg, Al, Si), and heavy (Mn, Fe, Co) masses in PCRs. For this analysis, data is simulated with QGSJET-II-04 and FLUKA hadronic interaction models for high and low energy, respectively. The data is generated in the energy range from 1 TeV to 10 PeV, which divide into 20 logarithmic bins with equal width of 0.2, see section 3.1 of [5] for details. In each energy bin, EASs are simulated in a zenith angle range from 0° to 45°, assuming a power law with a differential spectral index of −2.5. For the analysis, each shower is processed by throwing in a circular area of radius 150 m from the center (-13.85 m, 6.29 m) of the GRAPES-3 EAS array with a random core position. Each shower is reused ten times to improve the statistics. This dataset suffers from limited statistics at higher energy due to the steeply falling flux of CRs. Therefore, another dataset is generated with ten random core locations in a circular area of 60 m from the center of the array.

A detailed simulation study is done to calculate the trigger and reconstruction efficiencies, acceptance of the GRAPES-3 array, hadron punch-through, muon saturation, contribution of unassociated muons, and energy resolution. A detailed GEANT4 simulation is carried out to study the response of the secondary particles in the muon telescope [5]. The top absorber filters out the soft component of the EAS. Therefore, for each triggered shower, the response of EAS muons and hadrons is measured in terms of PRCs hit by using the GEANT4 simulation. These PRCs hits are used to count the muon tracks in the muon telescope.

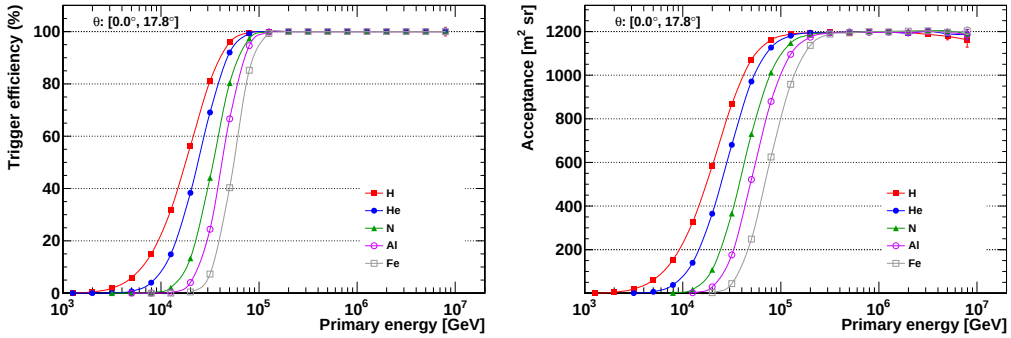

Figure 2: Trigger efficiency (left) and acceptance of GRAPES-3 scintillator detectors array (right) as a function of primary energy for $\theta < 18°$.

5. Analysis

5.1 Acceptance of the GRAPES-3 array

For each simulated primary, the trigger (ε_T) and reconstruction (ε_R) efficiencies are calculated as a function of primary energy, and total efficiency (ε_{tot}) is determined by the product of trigger and reconstruction efficiencies. Acceptance(A_{acc}) is represented as the product of the effective area and the effective viewing angle and defined as,

$$A_{acc}(E_T) = \frac{\pi A}{2}\varepsilon_{tot}(E_T)(cos2\theta_l - cos2\theta_u), \tag{1}$$

where A is the fiducial area and (θ_u, θ_l) are the upper and lower range of the zenith angle bin, respectively. The trigger efficiency and acceptance of all simulated primaries are shown in Figure 2. The trigger efficiency is >90% at 40 TeV, 45 TeV, 60 TeV, 70 TeV, and 85 TeV for H, He, N, Al, and Fe, respectively. The acceptance is increased to 1200 m^2 sr at 100% efficiency for $\theta < 18°$.

5.2 Estimation of mass composition

The muon multiplicity observed by the GRAPES-3 muon telescope is sensitive to the mass composition of the PCRs [6, 7]. Thus, the observed Muon Multiplicity Distribution (MMD) is utilized to estimate the relative composition of H, He, N, Al, and Fe without presuming the mass composition suggested by any composition model. The observed and simulated MMDs are corrected for the effect of muon saturation [5]. For the composition estimation, the observed and simulated MMDs are generated in a shower size (N_e) range from $10^{4.0}$ to $10^{6.0}$ with an equal bin-width of 0.2 on a logarithmic scale. The shape of simulated MMDs is well described by the negative binomial distribution (NBD). Therefore, the normalized MMD of each simulated primary is fitted with an NBD function to model the statistical uncertainties for each N_e bin. The left panel of Figure 3 shows the normalized MMDs of H and Fe, along with the fit curves, for $4.6 \leq \log(N_e) < 4.8$. The fitted mean (μ) and standard deviation (σ) exhibit a good agreement with the mean and standard deviation of the corresponding MMD. The normalized observed MMD is also plotted, and the MMDs of H and Fe (and corresponding fit curves) are scaled with 0.53 and 0.02, respectively, so that the lower and higher multiplicity of the observed MMD overlaps with the MMD of H and Fe,

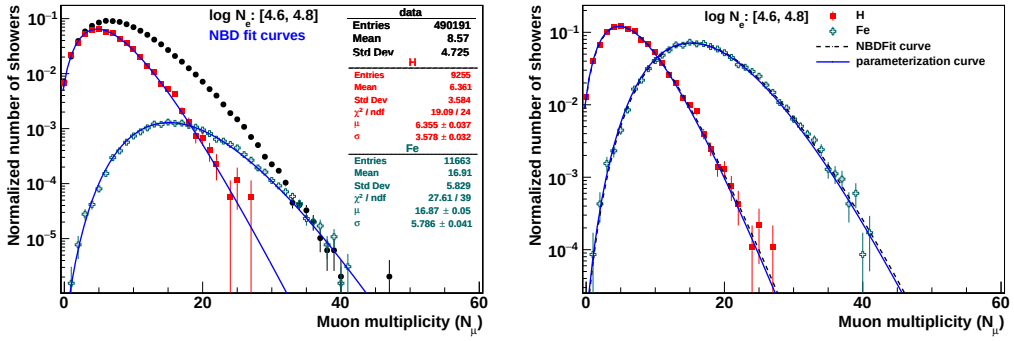

Figure 3: Left: Normalized MMD of the observed data (black circle) plotted along with MMDs of simulated primaries H (red square) and Fe (hollow cyan plus) for $4.6 \leq \log(N_e) < 4.8$. The blue curves represent the NBD fits. The MMDs of H and Fe, along with corresponding fit curves, are scaled to overlap with the tails of the observed MMD. Right: A comparison between the NBD curve obtained by fitting MMD with the NBD function (black dashed curve) and the NBD curve obtained using the μ and σ estimated from the parameterization (blue curve) for H and Fe primaries and $4.6 \leq \log(N_e) < 4.8$.

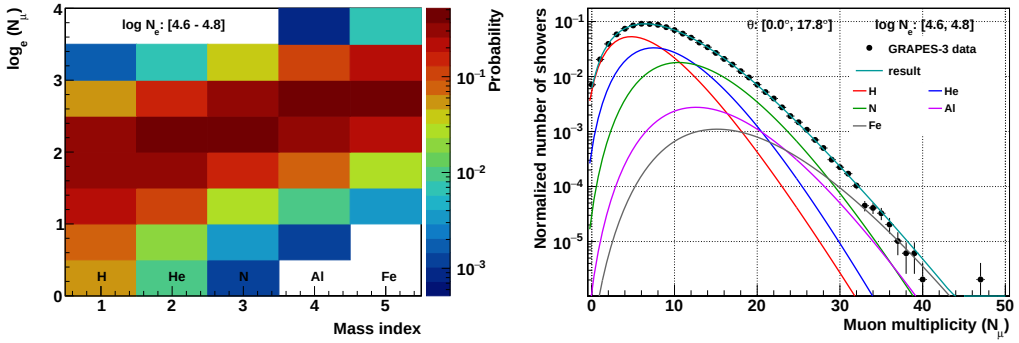

Figure 4: Left: Response matrix ($\mathbf{R_1}$) for $4.6 \leq \log(N_e) < 4.8$. The color gradient represents the probability of an EAS initiated by a given simulated primary having the $\log_e(N_\mu)$ value. Right: Comparing the normalized observed MMD (black circles) with the resultant curve (cyan curve) obtained by adding the MMD curves of all simulated primaries (different colored curves) scaled by their relative composition estimated from the Gold's unfolding, for $4.6 \leq \log(N_e) < 4.8$.

respectively. The lower and higher multiplicity of the observed MMD is well described by the H and Fe, respectively. However, primaries of the intermediate-mass group are required to describe the middle range of the observed MMD.

The fitted μ and σ exhibit a systematic increase with the shower size. Thus, the variation of μ and σ with N_e is further parameterized with a linear and a second-order polynomial function, and the fit parameters, along with the NBD function, are used to obtain the simulated MMD for a given shower size bin. The right panel of Figure 3 compares the NDB curve obtained from fitting (represented by the black dashed curve) and the NBD curve obtained by utilizing the μ and σ estimated from the parameterization (represented by the blue curve) for H and Fe primaries and $4.6 \leq \log(N_e) < 4.8$. Both curves show very good agreement with each other for both primaries.

In this analysis, the unfolding procedure is employed twice. In the first step, the unfolding procedure is utilized to estimate the relative composition of each primary group from the observed

MMD for each N_e bin. Subsequently, the energy spectrum of the proton primary is unfolded from the corresponding N_e distribution. Gold's unfolding algorithm [8] is used to estimate the relative composition of the simulated primary groups. The i^{th} element of the observed muon multiplicity vector ($\vec{N}_\mu$) represents the number of EASs in the i^{th} bin of the observed MMDs. The response matrix ($\mathbf{R_1}$) contains the probability values such that $R_{i,j}$ represents the probability of an EAS initiated by the j^{th} simulated primary having the muon multiplicity value belongs to i^{th} bin of the MMD. The $\mathbf{R_1}$ for $4.6 \leq \log(N_e) < 4.8$ is shown in the left panel of Figure 4, where the color gradient represents the probability values. Gold's algorithm is an iterative method, and the composition vector at the $(k+1)^{th}$ iteration ($\vec{A}^{k+1}$) is estimated from its previous estimate ($\vec{A}^{k}$) as,

$$A_i^{k+1} = A_i^k \frac{(\mathbf{R_1}^T \mathbf{C}^T \mathbf{C} \vec{N}_\mu)_i}{\sum_{j=1}^{5} (\mathbf{R_1}^T \mathbf{C}^T \mathbf{C} \mathbf{R_1})_{ij}\, A_j^k}, \tag{2}$$

where $\mathbf{C}$ is the error matrix for the observed data such that $C_{i,j} = \delta_{i,j} / N_{\mu,i}$ and δ is Kronecker delta. The relative composition proposed by the GST model is used as the prior for the unfolding. The criteria of a minimum of Weighted Mean Square Error (WMSE) [9] is used to obtain the optimal stopping iteration. A comparison of the normalized observed MMD with the resultant curve obtained by adding the MMD curves of all simulated primaries weighted by their relative composition estimated from the unfolding procedure is shown in the right panel of Figure 4 for $4.6 \leq \log(N_e) < 4.8$. Both show a good agreement with each other. The weighted NBD curves corresponding to the simulated primaries are also displayed.

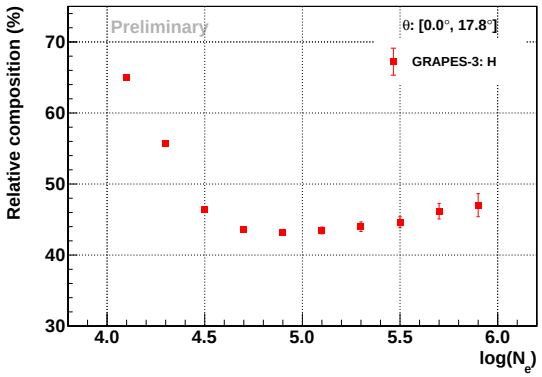

Figure 5: Relative composition of the proton primary obtained from the GRAPES-3 data as a function of the shower size. The error bars represent the statistical error.

The relative composition is found to be 65% at $N_e = 10^{4.1}$, decrease to 47% at $N_e = 10^{5.9}$, as shown in Figure 5. The statistical uncertainty increases from 0.3% to 3.5% for N_e range $10^{4.1}$ - $10^{5.9}$.

6. CR proton energy spectrum

The shower size distribution of the proton primary is obtained by weighting the number of EASs in a given shower bin of the observed shower size distribution with the relative composition of the proton obtained in the previous step. Gold's unfolding algorithm is used again to unfold the proton shower size distribution to the corresponding energy distribution. The optimal stopping iteration is identified by utilizing the criteria of minimum WMSE. Smoothing is applied to the unfolded energy distribution after each iteration, while the energy distribution at the optimal iteration is not smoothened. The differential cosmic-ray spectrum (Φ) can be expressed as follows,

$$\Phi(E_i) = \frac{1}{T_{live}} \left(\frac{N_i}{\Delta E_i \cdot A_{acc}(E_i)} \right), \tag{3}$$

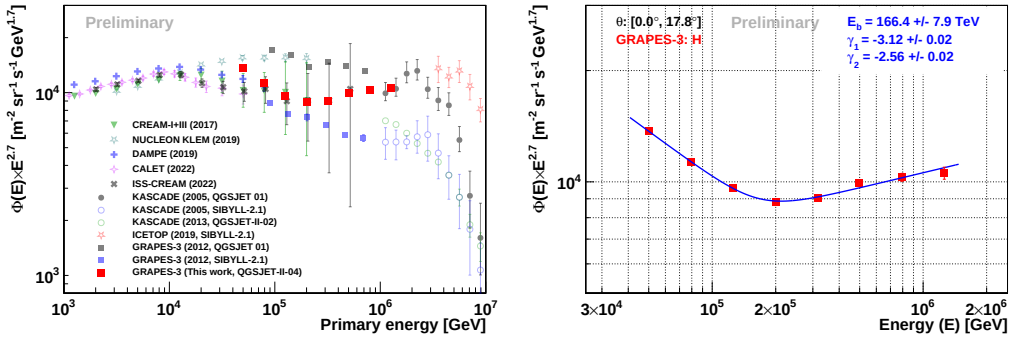

Figure 6: Left: A comparison between the proton energy spectrum obtained from the GRAPES-3 data in this work and those obtained by different direct and indirect experiments. Right: Modeling of the observed proton energy spectrum with a smoothly broken power law function.

where N_i, $A_{acc,1}$ and ΔE are the number of EAS, acceptance, and width of i^{th} energy bin of the unfolded energy distribution, respectively, and T_{live} is the live time of the data. In the left panel of Figure 6, the measured preliminary energy spectrum of the proton primary is plotted with direct [10–15] and indirect [16–18] observations. The flux of the measured proton spectrum in this work shows good agreement with ISS-CREAM, CREAM I+III at lower energy and is consistent with KASCADE (QGSJET-I-01) at higher energy. The proton energy spectrum exhibits a spectral hardening at around 165 TeV. The spectral hardening is modeled with a smoothly broken power law function, as shown in the right panel of Figure 6. The spectral hardening is found to be at 166 ± 8 TeV with spectral indices -3.12 ± 0.02 and -2.56 ± 0.02 before and after the energy break.

7. Acknowledgements

We thank D.B. Arjunan, A.S. Bosco, V. Jeyakumar, S. Kingston, N.K. Lokre, K. Manjunath, S. Murugapandian, S. Pandurangan, B. Rajesh, R. Ravi, V. Santhoshkumar, S. Sathyaraj, M.S. Shareef, C. Shobana, and R. Sureshkumar for their role in the efficient running of the experiment. We acknowledge the support of the Department of Atomic Energy, Government of India, under Project Identification No. RTI4002. This work was partially supported by grants from Chubu University and ICRR of Tokyo University, Japan.

References

[1] S. K. Gupta *et* al., GRAPES-3-A high-density air shower array for studies on the structure in the cosmic-ray energy spectrum near the knee, Nucl. Instrum. Meth. A **540**, 311 (2005).

[2] P. K. Mohanty *et* al., Measurement of some EAS properties using new scintillator detectors developed for the GRAPES-3 experiment, Astropart. Phys. **31**, 24 (2009).

[3] Y. Hayashi *et al.*, A large area muon tracking detector for ultra-high energy cosmic ray astrophysics-the GRAPES-3 experiment, Nucl. Instrum. Methods Phys. A **545**, 643 (2005).

[4] V. B. Jhansi *et al.*, The angular resolution of GRAPES-3 EAS array after improved timing and shower front curvature correction based on age and size, J. Cosmol. Astropart. Phys. **7**, 24 (2020).

[5] F. Varsi *et al.*, A GEANT4 based simulation framework for the large area muon telescope of the GRAPES-3 experiment, JINST, **18** P03046 (2023).

[6] H. Tanaka *et al.*, Studies of the energy spectrum and composition of the primary cosmic rays at 100–1000 TeV from the GRAPES-3 experiment, J. Phys. G: Nucl. Part. Phys. **39**, 025201 (2012).

[7] F. Varsi *et al.*, Updated results on the cosmic ray energy spectrum and composition from the GRAPES-3 experiment, SciPost Phys. Proc. (accepted).

[8] R. Gold, An iterative unfolding method for response matrices, Argonne National Laboratory, USA, **Rep. ANL-6984**, (1964).

[9] G. Cowan, Statistical Data Analysis, Clarendon Press, Oxford, 1998.

[10] A. D. Panov *et al.*, Energy spectra of abundant nuclei of primary cosmic rays from the data of ATIC-2 experiment: Final results, Bull. Russ. Acad. Sci. Phys. **73**, 564 (2009).

[11] Y. S. Yoon *et al.*, Proton and Helium Spectra from the CREAM-III Flight, Astrophys. J. **839**, 5 (2017).

[12] V. Grebenyuk *et al.*, Energy spectra of abundant cosmic-ray nuclei in the NUCLEON experiment, Adv. Space Res. **64**, 2546 (2019).

[13] Q. An *et al.*, Measurement of the cosmic ray proton spectrum from 40 GeV to 100 TeV with the DAMPE satellite, Sci. Adv. **5**, eaax3793 (2019).

[14] O. Adriani *et al.*, Observation of Spectral Structures in the Flux of Cosmic-Ray Protons from 50 GeV to 60 TeV with the Calorimetric Electron Telescope on the International Space Station, Phys. Rev. Lett. **129**, 101102 (2022).

[15] G. H. Choi *et al.*, Measurement of High-energy Cosmic-Ray Proton Spectrum from the ISS-CREAM Experiment, Astrophys. J. **940**, 107 (2022).

[16] T. Antoni *et al.*, KASCADE measurements of energy spectra for elemental groups of cosmic rays: Results and open problems, Astropart. Phys. **24**, 1 (2005).

[17] W. D. Apel *et al.*, KASCADE-Grande measurements of energy spectra for elemental groups of cosmic rays, Astropart. Phys. **47**, 54 (2013).

[18] M. G. Aartsen *et al.*, Cosmic ray spectrum and composition from PeV to EeV using 3 years of data from IceTop and IceCube, Phys. Rev. D **100**, 082002 (2019).